



Effect of detuning on the phonon induced dephasing of optically driven InGaAs/GaAs quantum dots

A. J. Ramsay, T. M. Godden, S. J. Boyle, E. M. Gauger, A. Nazir, B. W. Lovett, Achanta Venu Gopal, A. M. Fox, and M. S. Skolnick

Citation: *Journal of Applied Physics* **109**, 102415 (2011); doi: 10.1063/1.3577963

View online: <http://dx.doi.org/10.1063/1.3577963>

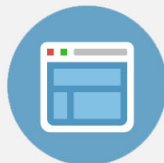
View Table of Contents: <http://scitation.aip.org/content/aip/journal/jap/109/10?ver=pdfcov>

Published by the [AIP Publishing](#)



Re-register for Table of Content Alerts

Create a profile.



Sign up today!



Effect of detuning on the phonon induced dephasing of optically driven InGaAs/GaAs quantum dots

A. J. Ramsay,^{1,a)} T. M. Godden,¹ S. J. Boyle,¹ E. M. Gauger,² A. Nazir,³ B. W. Lovett,² Achanta Venu Gopal,⁴ A. M. Fox,¹ and M. S. Skolnick¹

¹*Department of Physics and Astronomy, University of Sheffield, Sheffield, S3 7RH, United Kingdom*

²*Department of Materials, University of Oxford, Oxford OX1 3PH, United Kingdom*

³*Department of Physics and Astronomy, University College London, London, WC1E 6BT, United Kingdom*

⁴*DCMP & MS, Tata Institute of Fundamental Research, Mumbai 400 005, India*

(Received 25 July 2010; accepted 30 November 2010; published online 31 May 2011)

Recently, longitudinal acoustic phonons have been identified as the main source of the intensity damping observed in Rabi rotation measurements of the ground-state exciton of a single InAs/GaAs quantum dot. Here we report experiments of intensity damped Rabi rotations in the case of detuned laser pulses. The results have implications for the coherent optical control of both excitons and spins using detuned laser pulses. © 2011 American Institute of Physics. [doi:10.1063/1.3577963]

I. INTRODUCTION

The crystal ground and neutral exciton states of a single semiconductor quantum dot form a two-level system. As such, resonant excitation of the neutral exciton transition with a laser pulse drives an oscillation in the population inversion known as a Rabi oscillation.^{1,2} A Rabi rotation is typically measured by controlling the pulse-area, the time-integral of the Rabi frequency, via the incident power of the picosecond laser pulse. In the experiments the Rabi rotation is intensity damped, marking a strong departure from a two-level atom model, provoking a strong debate in the literature concerning the origins of the intensity damping.

In recent experiments, we have identified longitudinal acoustic phonons as the principal source of intensity damping of the ground-state (s-shell) transition of an InAs/GaAs self-assembled dot.³ We have further demonstrated that the fluctuations in the phonon bath give rise to a temperature and driving field dependent renormalization of the Rabi frequency, and a nonmonotonic decay of the Rabi oscillations due to the finite size of the quantum dot.⁴ Here we discuss the underlying physics of the interplay between a driven quantum dot and its phononic environment, and present experiments showing how the LA-phonons modify the absorption spectrum of a picosecond laser pulse.

II. WHAT IS INTENSITY DAMPING?

Figure 1 presents a Rabi rotation measurement taken at 5 K. A circularly polarized Gaussian laser pulse excites the neutral exciton transition of a single InAs/GaAs quantum dot on-resonance. The photocurrent which is proportional to the final exciton population is measured as a function of the square-root of the time-averaged incident power, \sqrt{P} . The x-axis is expressed in terms of the pulse-area $\Theta = \int_{-\infty}^{\infty} \Omega(t') dt' = a\sqrt{P}$, where the Rabi frequency of the pulse is described by $\Omega(t) = \Theta/(2\tau\sqrt{\pi}) \exp[-(t/2\tau)^2]$, $\tau = 4$ ps, and a is a measure of the dot-laser coupling. The dot-laser coupling, a , is

deduced from fits to Eqs. (2) and (3). Even at this low temperature, the resulting oscillation is damped with increasing power. For full details of the device and setup see Ref. 5.

To appreciate the relative unimportance of the conventional exponential-type dephasing, the dashed-trace in Fig. 1 presents a calculation of the Rabi rotation using a two-level model with a constant driving-field independent rate of dephasing $\Gamma_2^* = 0.025$ ps⁻¹. The dashed-trace is scaled to best fit the data, and hence the turning points do not occur at integer- π pulse-areas. Since the time duration of the pulse is constant, there is a fixed damage to the coherence, and the contrast is lost over the first period of the oscillation, but thereafter is almost constant. By comparison, the data is strongly damped. The damping is nonmonotonic, with the rate of damping decreasing with increasing solid-trace pulse-area, and the rotation angle is a nonlinear function of the pulse-area, exhibiting a decrease with pulse-area. The solid-trace is calculated using the model in the supplement of Ref. 3.

III. SUMMARY OF MODEL

For the sake of discussion, a summary of the model is presented here. For a full derivation of the model the reader is referred to the supplement of Ref. 3 and Refs. 6 and 7. The phonon-induced dephasing of an optically driven quantum dot has been the subject of a strong body of theoretical research.⁸⁻¹⁴ A number of alternative approaches for calculating the dephasing have been studied, including a numerically exact approach.¹⁵ Our model treats the quantum dot as an optically driven two-level system coupled to a bath of bosons, in this case LA-phonons. A transformation from the exciton basis to the optically dressed states, the energy eigen-states of the optically driven two-level system, results in a stationary frame where the exciton-phonon interaction is treated as a second-order perturbation. The main approximations are that the phonons are in thermal equilibrium, and a Born-Markov approximation which assumes that the exciton dynamics are slow compared to the lifetime or memory of the correlation function of the phonon bath $K(t)$. The end result is an intuitive, easy to use model described by a set of three Bloch

^{a)}Author to whom correspondence should be addressed. Electronic mail: a.j.ramsay@shef.ac.uk.

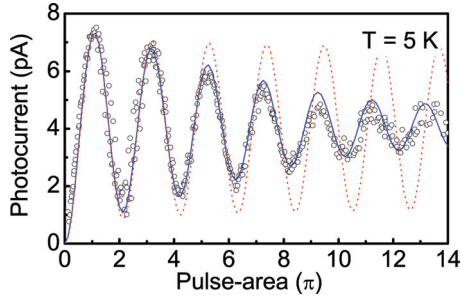


FIG. 1. (Color online) (◦) A Rabi rotation measurement at 5 K. Photocurrent vs square-root of incident power scaled to pulse-area of solid-trace. (red-dashed) Calculation of Rabi rotation using the two-level model with a pure dephasing rate of $\Gamma_2^* = 0.025 \text{ ps}^{-1}$. (blue-solid) Fit using LA-phonon model described in Sec. III.

equations, with additional Rabi-frequency dependent terms due to the phonon interaction

$$\dot{s}_x = \Delta s_y - \frac{\Omega^2 \Re[K(\Lambda)]}{\Lambda^2} s_x - \frac{\Delta \Omega \Re[K(\Lambda)]}{\Lambda^2} s_z - \frac{\pi \Omega J(\Lambda)}{2\Lambda}, \quad (1)$$

$$\dot{s}_y = \Omega \left(1 + \frac{\Im[K(\Lambda)]}{\Lambda} \right) s_z - \Delta s_x - \frac{\Omega^2 \Re[K(\Lambda)]}{\Lambda^2} s_y, \quad (2)$$

$$\dot{s}_z = -\Omega s_y. \quad (3)$$

The density-matrix is described by the Bloch-vector $\mathbf{s} = (s_x, s_y, s_z)$, where s_x and s_y represent the real and imaginary parts of the excitonic dipole and s_z represents the population inversion between the exciton and crystal ground-state. The Rabi frequency Ω and detuning of the laser $\Delta = \omega_X - \omega_{\text{laser}}$ result in an effective Rabi frequency, $\Lambda = \sqrt{\Omega^2 + \Delta^2}$. The exciton-phonon interaction gives rise to additional terms described by

$$\tilde{K}(t) = \int_0^\infty d\omega J(\omega) (2N(\omega) + 1) \cos(\omega t), \quad (4)$$

$$K(\Omega) = \int_0^\infty dt \tilde{K}(t) e^{i\Omega t}, \quad (5)$$

and the spectral density of the carrier-phonon interaction is

$$J(\omega) = \sum_{\mathbf{q}} |g_{\mathbf{q}}|^2 \delta(\omega - \omega_{\mathbf{q}}), \quad (6)$$

where $g_{\mathbf{q}}$ is a generic coupling strength of the exciton to a phonon of wave-vector \mathbf{q} . In the case of LA-phonons $g_{\mathbf{q}}$ is (Ref. 16)

$$g_{\mathbf{q}} = \frac{q \{ D_e \mathcal{P}[\psi^e(\mathbf{r})] - D_h \mathcal{P}[\psi^h(\mathbf{r})] \}}{\sqrt{2\mu\hbar\omega_{\mathbf{q}}V}}, \quad (7)$$

where μ is the mass density of the host material, V is the lattice volume, $D_{e(h)}$ is the respective bulk electron (hole) coupling constant, and $\mathcal{P}[\psi^{e(h)}]$ denotes the form factor of the electron (hole) wavefunction.

IV. INTERPRETATION OF MODEL: ZERO DETUNING

$\Delta = 0$

Here we consider the case of a Rabi rotation measurement where a single laser pulse excites the neutral exciton

transition on-resonance ($\Delta = 0$), with the dot initially in the crystal ground-state $\mathbf{s} = (0, 0, -1)$. In this case the Bloch Eqs. (1)–(3) simplify to

$$\dot{s}_y = \Omega \left(1 + \frac{\Im[K(\Omega)]}{\Lambda} \right) s_z - \Re[K(\Omega)] s_y, \quad (8)$$

$$\dot{s}_z = -\Omega s_y, \quad (9)$$

where the phonon interaction is described by a complex response function $K(\Omega)$. The real part describes a Rabi energy dependent rate of pure dephasing, and the imaginary term describes a phonon induced shift, or renormalization of the Rabi energy. The real and imaginary parts satisfy a Kramers-Kronig relation.

Figure 2 presents temperature dependent calculations of the phonon response function $K(\Omega)$ for the ground-state excitation transition of an InAs/GaAs quantum dot. To calculate $K(\Omega)$ the spectral density of the exciton-phonon interaction is approximated as $J(\omega) = \alpha\omega^3 e^{-\omega^2/\omega_c^2}$, where $\alpha = 0.0272 \text{ ps}^2$, and the cut-off energy is $\hbar\omega_c = 1.44 \text{ meV}$ as measured in Ref. 4. This approximation assumes the electron and hole have identical spherical Gaussian wavefunctions, and assumes the phonon modes are those of the bulk host material, in this case GaAs, resulting in a form-factor $\mathcal{P}[\psi^{e,h}(\mathbf{r})] \approx e^{-\omega^2/2\omega_c^2}$ in Eq. (6).

The real-part $\Re[K(\Omega)] = (\pi/2)\alpha\Omega^3 e^{-\Omega^2/\omega_c^2} \coth(\hbar\Omega/2k_B T)$ gives rise to a rate of pure dephasing, and is calculated in Fig. 2(a). In a low driving-field regime at absolute zero, the rate of dephasing scales with the driving-field cubed ($\lim_{\Omega \rightarrow 0, T \rightarrow 0} \Re[K] = \pi\alpha\Omega^3/2$). Whereas at high temperature, in the low driving-field regime, the rate of dephasing is proportional to the square of the driving-field, and the temperature ($\lim_{\Omega \rightarrow 0, T \rightarrow \infty} \Re[K] = \pi\alpha k_B T \Omega^2 / \hbar \equiv AT\Omega^2$).³ The exciton-phonon interaction has a finite energy bandwidth characterized by a cut-off energy that corresponds to the energy of a phonon with a wavelength equal to the size of the carrier wavefunction. At high driving-fields exceeding the cut-off energy, the coupling to the phonons with a high energy equal to the Rabi energy is weak, and the phonon-induced dephasing is suppressed. At intermediate driving-fields, this results in a roll-off

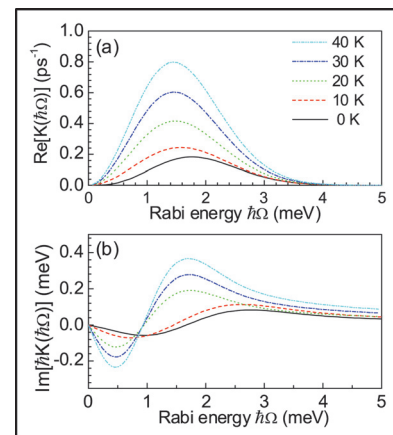


FIG. 2. (Color online) Rabi energy and temperature dependence of the exciton-phonon response, $K(\Omega)$. (a) The real-part gives a driving-field dependent rate of pure dephasing. (b) The imaginary part gives a renormalization of the Rabi energy.

in the rate of intensity damping at higher pulse-areas,⁴ and, in theory, the reappearance of high contrast Rabi oscillations at the high pulse-area as predicted in Refs. 6 and 15. Even at absolute zero, the dephasing due to the interplay between the driving field and the LA-phonons can be intense with a peak rate of dephasing of $\Re[K_{\max}] = 1/(5.6 \text{ ps})$.

The imaginary part of the phonon response $\Im[K]$ can be calculated numerically as shown in Fig. 2(b). This term gives rise to a shift in the rotation speed of the Bloch-vector from $\Omega \rightarrow \Omega_{\text{eff}} = \Omega\sqrt{1 + \Im[K(\Omega)]/\Omega}$, and acts as a rotation that causes an elliptical, rather than a circular, orbit of the Bloch-vector, where the ellipse is squeezed along the s_z -axis of the Bloch-sphere. The driving-field dependence of $\Im[K]$ gives rise to the nonperiodicity of the Rabi rotations observed in Ref. 4. In a low driving-field regime the effective optical dipole, which we define as $M = \lim_{\Omega \rightarrow 0} (\Omega_{\text{eff}}/\Omega)$ can be calculated as $M = \sqrt{1 - \int_0^\infty d\omega (J(\omega)/\omega^2) \coth(\hbar\omega/2k_B T)}$. At absolute zero the phonon interaction reduces the effective optical dipole by about 3%. The effective dipole decreases with temperature, explaining the increase in the period of the Rabi rotations with temperature observed in Ref. 4.

A physical picture of the driven phonon dephasing is as follows. The laser drives the charge state of the quantum dot at the Rabi frequency Ω . In turn, the modulation in the charge drives the lattice, resonantly coupling to phonons of the Rabi energy. The frequency dependence of the exciton-phonon coupling, due in part to the density of states, gives rise to a driving-field dependent rate of dephasing and a shift to the rotation angle described by $K(\Omega)$.

A complementary picture based on the model is that the laser couples the exciton states to form optically dressed states separated by the Rabi energy. Absorption and emission of phonons with an energy equal to the Rabi energy causes relaxation (second-order process) between the dressed states, which is interpreted as a dephasing process in the exciton basis. An experimental visualization of Rabi-split optically dressed states in the time-domain is presented in Ref. 17. This physical picture may be more general. Recent theoretical work suggests that near the band-edge of optical waveguides the radiative decay rate depends upon the driving field due to the Rabi side-bands feeling the strong energy gradient in the photon density of states.¹⁸ Similar effects have also been suggested in Ref. 19.

V. INFLUENCE OF DETUNING

Our understanding of the phonon-induced dephasing of an optically driven quantum dot has been experimentally tested in Refs. 3 and 4. Here we examine the role of detuning by studying the effect of the exciton-phonon interaction on the absorption spectrum of a picosecond laser pulse. A number of coherent optical control strategies use detuned,²⁰ or chirped laser pulses.^{21,22} In particular, coherent optical control schemes for a carrier spin usually rely on using detuned laser pulses to minimize the creation of the trion state (see, for example, Refs. 23 and 24). Hence, it is also important to understand intensity damping in the case of detuned laser pulses.

In the experiment, a single Gaussian laser pulse of $\tau = 4 \text{ ps}$ excites the quantum dot. A series of photocurrent spectra versus pulse-area are measured by tuning the laser frequency through the ground-state neutral exciton transition. The results are presented in the gray scale plot of Fig. 3(a). A peak that closely resembles the spectrum of the laser pulse is modulated by an oscillation in the pulse-area. This peak sits on top of a broad asymmetric feature.

Figure 3(b) presents a calculation of the photocurrent using $\alpha = 0.0272 \text{ ps}^2$ and $\hbar\omega_c = 1.44 \text{ meV}$ as determined by the on-resonance experiments.⁴ The pulse-area of Fig. 3(a) is scaled to match the model, which reproduces the data quite well. To aid the interpretation, the inset of Fig. 3(b) shows a calculation in the case of an ideal two-level system. The broad asymmetric feature arises from photon absorption that is assisted by the emission or absorption of an LA-phonon. At low temperatures, when the LA-phonon population is weak, the emission process is stronger resulting in stronger absorption of the blue-detuned laser. This asymmetry is described by the J-term in Eq. (1). A broad shoulder to the quantum dot line shape due to phonons has also been observed in CW-photoluminescence measurements.^{25,26}

In the case of the ideal two-level atom, the 3π -peak has a slight arrow-head like shape. The exciton-phonon interaction appears to accentuate the arrow-head. For a pulse-area of 2π the photocurrent spectra develops wings. We note that this effect was reported by Beham *et al.*,²⁷ but was not explained. As the detuning of the 2π -pulse, and hence, the effective Rabi frequency Λ is increased, the rate of dephasing increases. Consequently, the final state of the Bloch-

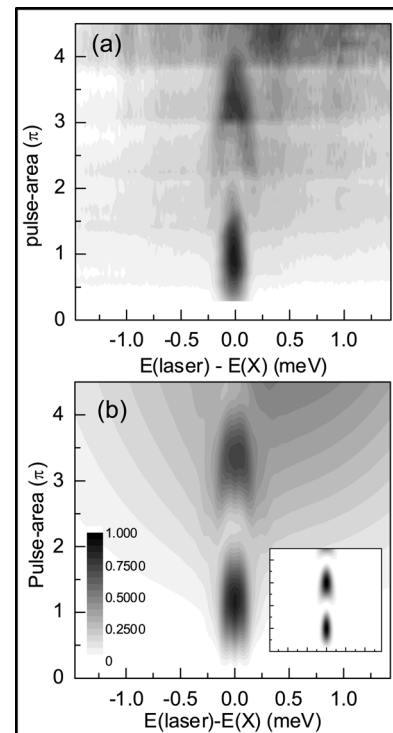


FIG. 3. (a) Gray scale plot of photocurrent of a single quantum dot excited by Gaussian pulse of $\tau = 4 \text{ ps}$ measured as a function of both laser detuning and pulse-area. The temperature is 15 K, and the reverse bias is 0.6 V. The photocurrent is scaled so that $1 \equiv 7.67 \text{ pA}$. (b) Calculation of photocurrent using Eqs. (1)–(3). (Inset) Calculation without dephasing.

vector for the detuned pulse resides closer to the center of the Bloch-sphere than for the on-resonant laser pulse, resulting in higher absorption for the detuned pulse and the formation of the wings. The absorption spectra of a quantum dot excited by a rectangular spectrum laser pulse can also exhibit side-peaks corresponding to the edges of the pulse spectrum,²⁸ but this is not a factor here.

In this section, we have measured the quantum dot absorption spectrum of a Gaussian laser pulse for various pulse-areas. In addition to the intensity damping of the Rabi oscillation, the exciton-phonon interaction gives rise to a broad asymmetric line shape due to phonon-assisted absorption. The absorption spectra is well-described by the model. Based on the model, for small detuning the increase in the effective Rabi frequency enhances the excitation dephasing. To achieve high fidelity operations, the red-detuning of the laser pulse needs to exceed the cut-off energy.

VI. EVIDENCE FOR PHONON-MEDIATED EXCITATION INDUCED DEPHASING IN PREVIOUS EXPERIMENTS

The strength of the intensity damping is determined by the α -parameter which is a bulk property of the host material. Therefore the strength of the intensity damping for all quantum dots embedded in GaAs should be $\alpha_{\text{GaAs}} = 0.0272 \text{ ps}^2$, as measured in Refs. 3 and 4. In this section, we test this hypothesis by comparing the model to other experimental reports of excitation induced dephasing.

In Ref. 29, Stuffer *et al.* report a high quality Rabi rotation of the ground-state neutral exciton transition using photocurrent detection. We note that the model can reproduce the intensity damping using the experimental parameters given in Ref. 29 and $\alpha = 0.0272 \text{ ps}^2$. The cut-off energy was used as the only fitting parameter and a value of $\hbar\omega_c = 1.67 \text{ meV}$ was obtained. This corresponds to an exciton probability distribution with a FWHM of 4.7 nm, which is reasonable for an InAs/GaAs quantum dot.

Off-resonant excitation of the wetting layer states has also been suggested as a possible mechanism for the intensity damping.³⁰ In Ref. 30, the argument is supported by a fit to the data of Zrenner *et al.*² We note, however, that the strength of the damping used is consistent with LA-phonons at a temperature of 4 K. In Ref. 31, the intensity damping of Rabi rotations of p-shell excitons was described using a rate of dephasing $\Gamma_2 = w(\Theta/\pi\tau_p)^2$ where τ_p is the intensity FWHM of the sech-pulse used in the experiments, and $c = 0.135 \text{ ps}$. However, similar results can also be obtained for LA-phonons at a temperature of 5 K, and a cut-off energy of $\sim 1.3 \text{ meV}$, suggesting that LA-phonons make a significant contribution to the intensity damping even for p-shell excitons that are energetically close to the wetting layer states.

In experiments to observe an Autler-Townes doublet,³² a 10% increase in the exciton linewidth for Rabi energies of up to 120 μeV was reported. At 4.2 K, a Rabi energy of 120 μeV would give rise to a rate of excitation induced dephasing of 0.5 μeV , compared to the 5 μeV linewidth of the exciton transition. In measurements of a Rabi oscillation driven by a continuous wave laser with Rabi energies of $<40 \mu\text{eV}$, Flagg *et al.*³³ reported no evidence for excitation

induced dephasing. Based on our model, the expected excitation induced dephasing due to phonons would be 56 meV, which was not resolvable in those experiments.

To conclude this section, intensity damping due to LA-phonons is an intrinsic dephasing mechanism. The α -parameter that defines the strength of the damping depends upon the bulk acoustic properties of the host material. We have explored this by comparing the LA-phonon model to a number of previously reported experiments, and find that the LA-phonon model is consistent with many key observations of intensity dependent dephasing under resonant excitation conditions.

VII. OUTLOOK

For a solid-state qubit coupled to a phononic environment the rate of dephasing is not characterized by a static number, but depends strongly upon the driving field. Achieving high-fidelity quantum logic operations will not be achieved by simply using faster laser pulses, but by optimizing the coherent control scheme to minimize dephasing based upon an understanding of a driven qubit coupled to a bath. While the experiments reported here and in Refs. 3 and 4 provide strong support for the existing theories, several important aspects remain untested. For example, if the driving-field is strong enough, will the intensity damped Rabi rotation reappear?^{6,15} Also, can one observe consequences of the phonon bath memory?¹¹ Conversely, can the phonon bath be used as a resource? For example, could a laser driven quantum dot be used as a Rabi frequency tunable point source of LA-phonons, as a nanoscale heat pump,³⁴ or for state inversion?³⁵

ACKNOWLEDGEMENTS

The authors thank the EPSRC (UK) EP/G001642, the QIPIRC UK, and UK-India Education Research Initiative for financial support. A.N. is supported by the EPSRC, and B.W.L. by the Royal Society. We thank H.Y. Liu and M. Hopkinson for sample growth. A.J.R. thanks the Royal Society for a travel grant to attend ICPS.

¹T. H. Stievater, X. Li, D. G. Steel, D. Gammon, D. S. Katzer, D. Park, C. Piermarocchi, and L. J. Sham *Phys. Rev. Lett.* **87**, 133603 (2001).

²A. Zrenner, E. Beham, S. Stuffer, F. Findeis, M. Bichler, and G. Abstreiter, *Nature (London)* **418**, 612 (2002).

³A. J. Ramsay, A. V. Gopal, E. M. Gauger, A. Nazir, B. W. Lovett, A. M. Fox, and M. S. Skolnick, *Phys. Rev. Lett.* **104**, 017402 (2010).

⁴A. J. Ramsay, T. M. Godden, S. J. Boyle, E. M. Gauger, A. Nazir, B. W. Lovett, A. M. Fox, and M. S. Skolnick, *Phys. Rev. Lett.* **105**, 177402 (2010).

⁵S. J. Boyle, A. J. Ramsay, F. Bello, H. Y. Liu, M. Hopkinson, A. M. Fox, and M. S. Skolnick, *Phys. Rev. B* **78**, 075301 (2008).

⁶A. Nazir, *Phys. Rev. B* **78**, 153309 (2008).

⁷E. M. Gauger, S. C. Benjamin, A. Nazir, and B. W. Lovett, *Phys. Rev. B* **77**, 115322 (2008).

⁸J. Förstner, C. Weber, J. Dankwerts, and A. Knorr, *Phys. Rev. Lett.* **91**, 127401 (2003).

⁹P. Machnikowski and L. Jacak, *Phys. Rev. B* **69**, 193302 (2004).

¹⁰A. Krügel, V. M. Axt, T. Kuhn, P. Machnikowski, and A. Vagov, *Appl. Phys. B* **81**, 897 (2005).

¹¹A. Krügel, V. M. Axt, and T. Kuhn, *Phys. Rev. B* **73**, 035302 (2006).

¹²U. Hohenester and G. Stadler, *Phys. Rev. Lett.* **92**, 196801 (2004).

¹³V. M. Axt, P. Machnikowski, and T. Kuhn, *Phys. Rev. B* **71**, 155305 (2005).

¹⁴T. E. Hodgson, L. Viola, and I. D'Amico, *Phys. Rev. B* **78**, 165311 (2008).

- ¹⁵A. Vagov, M. D. Croitoru, V. M. Axt, T. Kuhn, and F. M. Peeters, *Phys. Rev. Lett.* **98**, 227403 (2007).
- ¹⁶B. Krummheuer, V. M. Axt, and T. Kuhn, *Phys. Rev. B* **65**, 195313 (2002).
- ¹⁷S. J. Boyle, A. J. Ramsay, A. M. Fox, M. S. Skolnick, A. P. Heberle, and M. Hopkinson, *Phys. Rev. Lett.* **102**, 207401 (2009).
- ¹⁸X. Ma and S. John, *Phys. Rev. Lett.* **103**, 233601 (2009).
- ¹⁹R. Melet, V. Voliotis, A. Enderlin, D. Roditchev, X. L. Wang, T. Guillet, and R. Grousson, *Phys. Rev. B* **78**, 073301 (2008).
- ²⁰T. Unold, K. Mueller, C. Lienau, T. Elsaesser, and A. D. Wieck, *Phys. Rev. Lett.* **92**, 157401 (2004).
- ²¹Y. Wu, I. M. Piper, M. Ediger, P. Brereton, E. R. Schmidgall, M. Hugues, M. Hopkinson, and R. T. Phillips, *Phys. Rev. Lett.* **106**, 067401 (2011).
- ²²C. M. Simon, T. Belhadj, B. Chatel, T. Amand, P. Renucci, A. Lemaitre, O. Krebs, P. A. Dalgarno, R. J. Warburton, X. Marie, and B. Urbaszek, arXiv:1007.2808.
- ²³D. Press, T. H. Ladd, B. Zhang, and Y. Yamamoto, *Nature (London)* **456**, 218 (2008).
- ²⁴D. Kim, S. G. Carter, A. Greilich, A. Bracker, and D. Gammon, *Nat. Phys.* **7**, 223 (2011).
- ²⁵L. Besombes, K. Kheng, L. Marsal, and H. Mariette, *Phys. Rev. B* **63**, 155307 (2001).
- ²⁶I. Favero, G. Cassabois, R. Ferreira, D. Darson, C. Voisin, J. Tignon, C. Delalande, G. Bastard, Ph. Roussignol, and J. M. Gérard, *Phys. Rev. B* **68**, 233301 (2003).
- ²⁷E. Beham, A. Zrenner, S. Stuffer, F. Findeis, M. Bichler, and G. Abstreiter, *Physica E* **16**, 59 (2003).
- ²⁸A. J. Ramsay, R. S. Kolodka, F. Bello, P. W. Fry, W. K. Ng, A. Tahraoui, H. Y. Liu, M. Hopkinson, D. M. Whittaker, A. M. Fox, and M. S. Skolnick, *Phys. Rev. B* **75**, 113302 (2007).
- ²⁹S. Stuffer, P. Ester, A. Zrenner, and M. Bichler, *Phys. Rev. B* **72**, 121301(R) (2005).
- ³⁰J. M. Villas-Bôas, S. E. Ulloa, and A. O. Govorov, *Phys. Rev. Lett.* **94**, 057404 (2005).
- ³¹Q. Q. Wang, A. Muller, P. Bianucci, E. Rossi, Q. K. Que, T. Takahara, C. Piermarocchi, A. H. MacDonald, and C. K. Shih, *Phys. Rev. B* **72**, 035306 (2005).
- ³²G. Jundt, L. Robledo, A. Högele, S. Fält, and A. Imamoglu, *Phys. Rev. Lett.* **100**, 177401 (2008).
- ³³E. B. Flagg, A. Muller, J. W. Robertson, S. Founta, D. G. Deppe, M. Xiao, W. Ma, G. J. Salamo, and C. K. Shih, *Nat. Phys.* **5**, 203 (2009).
- ³⁴E. M. Gauger, and J. Wabnig, *Phys. Rev. B* **82**, 073301 (2010).
- ³⁵T. M. Stace, A. C. Doherty, and S. D. Barrett, *Phys. Rev. Lett.* **95**, 106801 (2005).